Thermal Modeling

7.1: Introduction and preliminary definitions

- Up until now, we have assumed that the cell we are modeling is at a constant temperature.
- When considering thermal aspects of real cells, we must account for:
  1. Usage of a cell generates (or sinks) heat;
  2. Local heat addition/removal changes temperature at that location;
  3. Heat flows within cell and to/from environment at cell boundaries;
  4. Cell operational parameters are temperature dependent: cell works differently at different temperatures.
- For a coupled electrochemical-thermal model, we must be able to model each of these effects.

Preliminary definitions

- Temperature is a measure of the tendency of an object to give up energy to its surroundings spontaneously.
- When two objects are in thermal contact, the one that tends to lose energy spontaneously is at the higher temperature.
- If we are precise, we can write

$$\frac{1}{T} = \left(\frac{\mathrm{d}S}{\mathrm{d}U}\right)_{n,V},$$

relating temperature T to entropy S and internal energy U when the number of particles and volume are held constant.

- A simpler (but less precise) definition of temperature relates it to the translational kinetic energy associated with the disordered microscopic translational motion of atoms or molecules in a system.
- According to this definition of kinetic temperature,

$$\left[\frac{1}{2}mv^2\right]_{\text{average}} = \frac{3}{2}kT,$$

where k is the Boltzmann constant. While this definition has some problems, it will be sufficient to understand this chapter.

- Heat can be defined as "thermal energy in transit."
  - Heat flux refers to movement of thermal energy, which tends to change the temperatures of the source and destination.
  - Heat generation refers to thermal energy being added to a system, tending to increase its temperature.
  - A heat sink removes thermal energy from a system, tending to decrease its temperature.
- There are various mechanisms by which thermal energy can travel: conduction, convection, and radiation.

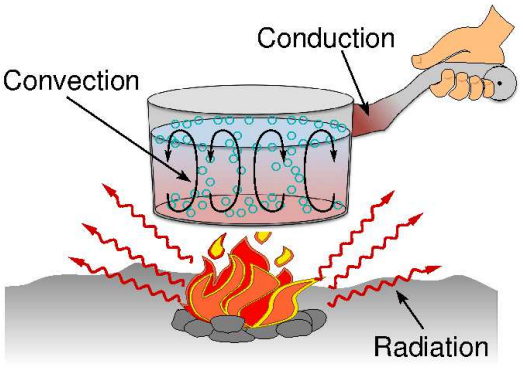

- Conduction transfers thermal energy within a system, as neighboring molecules impart/receive energy to/from each other.
- If you put a metal cooking pot over a fire, it will absorb the energy from the flame (via radiation energy transfer).

- The molecules absorbing the energy will vibrate more quickly, bumping into the molecules next to them, increasing their energy, etc.
- As this process continues, the heat is transferred from the part directly over the fire to the extremities of the pot.
- The ability of a material to conduct heat depends on its macroscopic and microscopic structure.
  - Styrofoam cups and double-paned windows are good thermal insulators because gas pockets do not conduct heat well.
  - Metals are good thermal conductors due to the tight internal bonding of their atoms.
- Convection is the transfer of thermal energy due to the mass movement of a fluid (liquid or gas) arising from a pressure gradient.
  - Natural convection occurs because warm fluids are less dense than cold fluids, so warm fluids tend to rise and cold fluids fall.
  - Forced convection relies on a fan or pump to augment the natural pressure gradient to speed fluid movement.
- An object is cooled via convection when a thin layer of fluid in contact with it is first heated via conduction.
  - Conduction alone does not account for the cooling, however, as fluids are generally poor conductors of thermal energy.
  - Instead, the thin layer of fluid heated by conduction caries the heat away from the system by convection.
  - This cycle repeats when a new cooler layer of fluid takes its place.
- Radiation is the transfer of thermal energy via electromagnetic waves.

  - Radiation doesn't require contact between the heat source and the heated object as is the case with both conduction and convection.
  - No mass is exchanged and no medium is required in the process of radiation: heat can be transmitted though empty space.
  - This energy is absorbed when these waves encounter an object.
  - For example, energy traveling from the sun to your skin: you can feel your skin getting warmer as energy is absorbed.

- Finally, we review the important thermodynamic potential enthalpy:
  - Enthalpy H is the total amount of energy stored by the system that could be released as heat. In a process,
    - If $\Delta H > 0$, system has received energy in the form of heat;
    - If $\Delta H < 0$, system has released energy in the form of heat;
  - So, ΔH must be proportional to Δq.
- Enthalpy is related to internal energy, but is not equal to internal energy because the First Law of thermodynamics states

$$\Delta U = \Delta q + \Delta w \neq \Delta q.$$

- To remove the Δw term, enthalpy is defined as $H = U + pV$ and is most useful for constant-pressure calculations:
  - Many chemical reactions occur under (constant) atmospheric pressure, so we may regard them as constant pressure processes.
  - The change in enthalpy is then the heat released by the reaction.

$$\mathrm{d}H = \mathrm{d}U + \mathrm{d}(pV) = \mathrm{d}U + p\,\mathrm{d}V + V\,\mathrm{d}p = \mathrm{d}U + p\,\mathrm{d}V$$

$$= \cancel{\mathrm{d}}q + \cancel{\mathrm{d}}w + p\,\mathrm{d}V = \cancel{\mathrm{d}}q - p\,\mathrm{d}V + p\,\mathrm{d}V = \cancel{\mathrm{d}}q.$$

7.2: Microscale thermal model

- With this introduction, we are ready to proceed to the rest of the microscale derivation, based on a paper by Gu and Wang.[1]
- For a multi-phase system, a general differential equation of thermal energy balance, based on first principles, is[2]

$$\rho_k c_{P,k}\left(\frac{\partial T_k}{\partial t}+\mathbf{v}_k\cdot\nabla T_k\right)=\nabla\cdot(\lambda_k\nabla T_k)-\sum_{\text{species } i}\mathbf{j}_{k,i}\cdot\nabla H_{k,i}.$$

- First term on left models energy storage (as increase in temperature):
  - ρ_k is the density of phase k [kg m^{-3}], $c_{P,k}$ is the specific heat of phase k [J kg^{-1} K^{-1}], T_k is temperature of phase k [K].
- Second term on left is a convection term—local energy changes because warmer or colder materials flow into the region of interest:
  - $\mathbf{v}_k$ is the average velocity of the mixture [m s^{-1}].
- First term on right models heat flux due to thermal diffusion:
  - λ_k is the thermal conductivity of phase k.
  - Conductivities of some categories of material are tabulated.
  - Battery materials have typical thermal conductivities around 5 W m^{-1} K^{-1}.

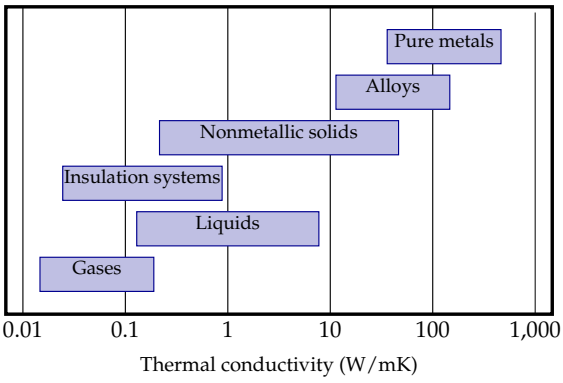

[1] W.B. Gu and C.Y. Wang, "Thermal-Electrochemical Modeling of Battery Systems," *Journal of the Electrochemical Society*, 147(8), 2910–2922 (2000).

[2] R.B. Bird, W.E. Stewart and E.N. Lightfoot, *Transport Phenomena*, second edition, John Wiley and Sons, 2002. This result is from Table 19.2-4, entry (F) in Bird's book, combined with Bird 19.3-6, as derived in Gu & Wang.

- Second term on right models heat flux due to material flux
  - $\mathbf{j}_{k,i}$ is the molar flux due to diffusion and migration of species i in phase k, relative to the mixture's average velocity [mol m^{-2} s^{-1}],
    - $H_{k,i}$ is the partial molar enthalpy of species i in phase k, where $H_{k,i} = U_{k,i} + pV_{k,i}$ [J mol^{-1}].
- We're going to assume that convection is negligible and drop it from the equation, giving:

$$\rho_k c_{P,k} \frac{\partial T_k}{\partial t} = \nabla \cdot (\lambda_k \nabla T_k) - \sum_{\text{species } i} \mathbf{j}_{k,i} \cdot \nabla H_{k,i}.$$

- Heat generation is a phenomena that occurs at the boundary between phases due to chemical reactions occurring there, and we will explore this in due course.

Evaluating the partial molar enthalpy term

- To proceed, we need to be able to work with the $H_{k,i}$ term.

$$\begin{aligned} H_{k,i} &= \left(\frac{\mathrm{d}H}{\mathrm{d}n_{k,i}} \right)_{T,p,n_{j\neq k,i}} \\ &= \left(\frac{\mathrm{d}(G+TS)}{\mathrm{d}n_{k,i}} \right)_{T,p,n_{j\neq k,i}} \\ &= \left(\frac{\mathrm{d}G}{\mathrm{d}n_{k,i}} \right)_{T,p,n_{j\neq k,i}} + T \left(\frac{\mathrm{d}S}{\mathrm{d}n_{k,i}} \right)_{T,p,n_{j\neq k,i}}. \end{aligned}$$

- Recall that the first term is equal to the electrochemical potential $\bar{\mu}_{k,i}$.
- To evaluate the second term, we need the Gibbs–Duhem relationship

$$S\mathrm{d}T - V\mathrm{d}p = -\sum_{i=1}^{r} n_i \mathrm{d}\bar{\mu}_i$$

$$S = V\frac{\mathrm{d}p}{\mathrm{d}T} - \sum_{i=1}^{r} n_i \frac{\mathrm{d}\bar{\mu}_i}{\mathrm{d}T}$$

$$\left(\frac{\mathrm{d}S}{\mathrm{d}n_{k,i}}\right)_{T,p,n_{j\neq k,i}} = -\frac{\mathrm{d}\bar{\mu}_{k,i}}{\mathrm{d}T}.$$

- Combining, we have,

$$H_{k,i} = \bar{\mu}_{k,i} - T\left(\frac{\mathrm{d}\bar{\mu}_{k,i}}{\mathrm{d}T}\right)_{p,n_j}.$$

- Now, recall one definition of the electrochemical potential,

$$\begin{aligned}
\bar{\mu}_k &= RT\ln(\lambda_k) + z_k F\phi_k \\
H_{k,i} &= RT\ln(\lambda_{k,i}) + z_{k,i}F\phi_{k,i} - T\frac{\mathrm{d}(RT\ln(\lambda_{k,i}) + z_{k,i}F\phi_{k,i})}{\mathrm{d}T} \\
&= RT\ln(\lambda_{k,i}) + z_{k,i}F\phi_{k,i} - T\frac{\mathrm{d}RT\ln(\lambda_{k,i})}{\mathrm{d}T} - z_{k,i}FT\frac{\mathrm{d}\phi_{k,i}}{\mathrm{d}T} \\
&= RT\ln(\lambda_{k,i}) - T\left(R\ln(\lambda_{k,i}) + RT\frac{\mathrm{d}\ln(\lambda_{k,i})}{\mathrm{d}T}\right) + z_{k,i}F\left(\phi_{k,i} - T\frac{\mathrm{d}\phi_{k,i}}{\mathrm{d}T}\right) \\
&= -RT^2\frac{\mathrm{d}\ln(\lambda_{k,i})}{\mathrm{d}T} + z_{k,i}F\left(\phi_{k,i} - T\frac{\mathrm{d}\phi_{k,i}}{\mathrm{d}T}\right).
\end{aligned}$$

- Continuing with the gradient term that we need,

$$\nabla H_{k,i} = -R\nabla\left(T^2\frac{\mathrm{d}\ln(\lambda_{k,i})}{\mathrm{d}T}\right) + z_{k,i}F\nabla\left(\phi_{k,i} - T\frac{\mathrm{d}\phi_{k,i}}{\mathrm{d}T}\right).$$

- The first term is closely related to the enthalpy of mixing, and is generally ignored in practice.
- We also generally ignore the temperature dependence of phase potential. Also, local potential of all species will be equal, so,

$$\nabla H_{k,i} = z_{k,i}F\nabla\phi_k.$$

- Substituting this into the prior relationship,

$$\rho_k c_{P,k} \frac{\partial T_k}{\partial t} = \nabla \cdot (\lambda_k \nabla T_k) - \sum_{\text{species } i} z_{k,i} F \mathbf{j}_{k,i} \cdot \nabla \phi_k.$$

- Noting that the current through phase k results from diffusion and migration of ionic species in the phase under the assumption of electroneutrality where

$$\mathbf{i}_k = \sum_{\text{species } i} z_{k,i} F \mathbf{j}_{k,i},$$

(in [A m^{-2}]), so we can rewrite the relationship as

$$\rho_k c_{P,k} \frac{\partial T_k}{\partial t} = \nabla \cdot (\lambda_k \nabla T_k) - \mathbf{i}_k \cdot \nabla \phi_k.$$

Boundary Conditions

- As we have seen, the PDE by itself must be accompanied by a suitable boundary condition in order to simulate the dynamics.
- Here, we are concerned about the solid–electrolyte boundary.
- In a nontrivial derivation,[3] $\lambda_e \nabla T_e \cdot \hat{\mathbf{n}}_e + \lambda_s \nabla T_s \cdot \hat{\mathbf{n}}_s = F j \eta + F j \Pi$.
- The left side of the expression is the sum of the heat flux into the electrolyte and into the solid [W m^{-2}].
- The right side is heat generation/sink at surface:
  - The $j\eta$ term models irreversible heat generation (always positive).
  - The $j\Pi$ term models reversible heat gen. (positive or negative).
- We will see how to evaluate these terms in the next section.

[3] J. Newman, "Thermoelectric Effects in Electrochemical Systems," *Ind. Eng. Chem. Res.*, 1995, 34, 3208–3216.

7.3: Continuum thermal model

- Our goal now is to volume average over the phases to get a continuum-scale equation. Starting with,

$$\rho_k c_{P,k} \frac{\partial T_k}{\partial t} = \nabla \cdot (\lambda_k \nabla T_k) - \mathbf{i}_k \cdot \nabla \phi_k.$$

- We use volume-averaging theorem 3 on the LHS of the equation, assuming that the solid–electrolyte phase boundary is not moving,

$$\rho_k c_{P,k} \overline{\left[\frac{\partial T_k}{\partial t} \right]} = \frac{1}{\varepsilon_k} \rho_k c_{P,k} \frac{\partial (\varepsilon_k \bar{T}_k)}{\partial t}.$$

- We use volume-averaging theorem 2 on the first term of the RHS,

$$\overline{\nabla \cdot (\lambda_k \nabla T_k)} = \frac{1}{\varepsilon_k} \left[\nabla \cdot (\varepsilon_k \overline{\lambda_k \nabla T_k}) + \frac{1}{V} \oiint_{A_{se}} (\lambda_k \nabla T_k) \cdot \hat{\mathbf{n}}_k \, \mathrm{d}A \right].$$

  - We model $\varepsilon_k \overline{\lambda_k \nabla T_k} \approx \lambda_{\text{eff},k} \nabla \bar{T}_k$, where $\lambda_{\text{eff},k} = \lambda_k \varepsilon_k^{\text{brug}}$, and assume that the integrand is constant within the small volume V,

$$\begin{aligned} \overline{\nabla \cdot (\lambda_k \nabla T_k)} &\approx \frac{1}{\varepsilon_k} \left[\nabla \cdot (\lambda_{\text{eff},k} \nabla \bar{T}_k) + \frac{A_{se} (\lambda_k \nabla T_k) \cdot \hat{\mathbf{n}}_k}{V} \right] \\ &= \frac{1}{\varepsilon_k} \left[\nabla \cdot (\lambda_{\text{eff},k} \nabla \bar{T}_k) + a_s (\lambda_k \nabla T_k) \cdot \hat{\mathbf{n}}_k \right]. \end{aligned}$$

- The second term on the RHS of the equation is more tricky, since we don't have a volume-averaging theorem to help with it. This term is handled by "completing the square." Consider,

$$(\mathbf{i}_k - \bar{\mathbf{i}}_k) \cdot (\nabla (\phi_k - \bar{\phi}_k)) = [\mathbf{i}_k \cdot \nabla \phi_k] - [\mathbf{i}_k \cdot \nabla \bar{\phi}_k] - [\bar{\mathbf{i}}_k \cdot \nabla \phi_k] + [\bar{\mathbf{i}}_k \cdot \nabla \bar{\phi}_k].$$

  - This allows us to write the term of interest as,

$$[\mathbf{i}_k \cdot \nabla \phi_k] = [\mathbf{i}_k \cdot \nabla \bar{\phi}_k] + [\bar{\mathbf{i}}_k \cdot \nabla (\phi_k - \bar{\phi}_k)] + (\mathbf{i}_k - \bar{\mathbf{i}}_k) \cdot (\nabla (\phi_k - \bar{\phi}_k)).$$

- We take volume averages of this equation term-by-term.

- Because $\nabla\bar{\phi}_k$ is a constant, the volume average of the first term is:

$$\overline{[\mathbf{i}_k \cdot \nabla\bar{\phi}_k]} = \frac{1}{V_k}\int_{V_k}[\mathbf{i}_k \cdot \nabla\bar{\phi}_k]\,\mathrm{d}V = \left(\frac{1}{V_k}\iiint_{V_k}\mathbf{i}_k\,\mathrm{d}V\right)\cdot\nabla\bar{\phi}_k = \bar{\mathbf{i}}_k \cdot \nabla\bar{\phi}_k.$$

- For the second term, we use volume-averaging theorem 1:

$$\overline{[\bar{\mathbf{i}}_k \cdot \nabla(\phi_k - \bar{\phi}_k)]} = \underbrace{\bar{\mathbf{i}}_k \cdot \nabla(\bar{\phi}_k - \bar{\phi}_k)}_{0} + \bar{\mathbf{i}}_k \cdot \frac{1}{V}\oiint_{A_{se}}(\phi_k - \bar{\phi}_k)\hat{\mathbf{n}}_k\,\mathrm{d}A,$$

  where Gu and Wang show that the integral term is small compared to the other terms, and so this entire expression is dropped.

- For the third term, we use the definition of volume averaging:

$$\overline{(\mathbf{i}_k - \bar{\mathbf{i}}_k)\cdot(\nabla(\phi_k - \bar{\phi}_k))} = \frac{1}{V_k}\iiint_{V_k}(\mathbf{i}_k - \bar{\mathbf{i}}_k)\cdot(\nabla(\phi_k - \bar{\phi}_k))\,\mathrm{d}V.$$

  Gu and Wang did not give any advice for how to evaluate this term, but omitted it from their final result, assuming it was negligible.

- Combining all results to date,

$$\frac{1}{\varepsilon_k}\rho_k c_{pk}\frac{\partial(\varepsilon_k\overline{T_k})}{\partial t} = \frac{1}{\varepsilon_k}\left[\nabla\cdot(\lambda_{\mathrm{eff},k}\nabla\bar{T}_k) + a_s(\lambda_k\nabla T_k)\cdot\hat{\mathbf{n}}_k\right] - \bar{\mathbf{i}}_k\cdot\nabla\bar{\phi}_k.$$

- We assume that local thermal equilibrium exists in the system,

$$\bar{T}_s = \bar{T}_e = T,$$

  and sum the above equation over the solid and electrolyte phases,

$$\frac{\partial(\rho c_P T)}{\partial t} = \nabla\cdot\lambda\nabla T + q,$$

  where

$$\rho c_P = \sum_{k\in\{s,e\}}\varepsilon_k\rho_k c_{P,k} \qquad \text{and} \qquad \lambda = \sum_{k\in\{s,e\}}\lambda_{\mathrm{eff},k},$$

  and the heat-source term q is given by

$$q = \sum_j a_{sj}F\bar{j}(\bar{\eta}_j + \bar{\Pi}_j) - \sum_k \varepsilon_k\bar{\mathbf{i}}_k\cdot\nabla\bar{\phi}_k.$$

- The Peltier coefficient was derived in Newman's paper to equal

$$\Pi_j = T\frac{\partial U_{\text{ocp},j}}{\partial T}.$$

  - The partial molar entropy $\partial U_{\text{ocp},j}/\partial T$ term has to do with change in OCP as temperature varies.
  - Plot shows representative curves.
  - At different stages of lithiation, more or less order is produced by lithiation, so heat is either generated or sunk.

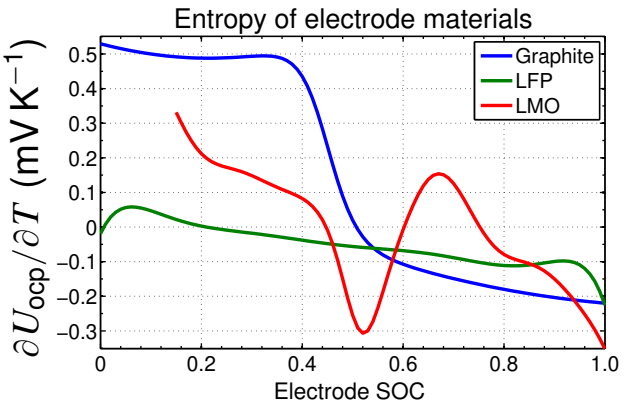

- Recall from notes chapter 4 that volume-averaged current density through solid and electrolyte phases are

$$\varepsilon_s \bar{\mathbf{i}}_s = -\sigma_{\text{eff}}\nabla\bar{\phi}_s \qquad \text{and} \qquad \varepsilon_e \bar{\mathbf{i}}_e = -\kappa_{\text{eff}}\nabla\bar{\phi}_e - \kappa_{D,\text{eff}}\nabla \ln \bar{c}_e.$$

- Summarizing (and removing over-lines from volume-averaged quantities to clean up notation), the heat-gen. terms [W m^{-3}] are:
  - Irreversible heat gen. $q_i = a_s F j_j \eta_j$ due to chemical reaction j,
  - Reversible heat gen. $q_r = a_s F j_j T\frac{\partial U_{\text{ocp},j}}{\partial T}$ due to change in entropy,
  - Joule heating in solid, $q_s = \sigma_{\text{eff}}(\nabla\phi_s \cdot \nabla\phi_s)$,
  - Electrolyte Joule heating, $q_e = \kappa_{\text{eff}}(\nabla\phi_e \cdot \nabla\phi_e) + \kappa_{D,\text{eff}}(\nabla \ln c_e \cdot \nabla\phi_e)$.
- We sometimes also include contact-resistance and current-collector heat generation, $q_c = i_{\text{app}}^2(R_{\text{contact}} + R_{\text{cc}})$ [W m^{-2}].
  - Note different units: Applies only to current-collector/electrode contact region, so is per unit area rather than per unit volume.

Transfer of heat at boundaries

- At the cell boundaries, there are three methods by which heat can be conducted into or out of the cell: convection, conduction, radiation.
- Conduction can be modeled as a fixed temperature specified at surface. In one dimension, we can write

$$T(x,t)|_{x=0} = T_0, \quad T(x,t)|_{x=L} = T_L.$$

- Conduction can also be modeled as a fixed heat flux at the surface.

$$-\lambda^{\text{eff}} \left.\frac{\partial T(x,t)}{\partial x}\right|_{x=0} = \mathbf{q}_0, \quad \lambda^{\text{eff}} \left.\frac{\partial T(x,t)}{\partial x}\right|_{x=L} = \mathbf{q}_L,$$

  where the sign of the derivatives flip at $x = L$ to reflect the convection of heat flux into the surface as positive.
- A special case is the adiabatic (or insulated) surface for which

$$\left.\frac{\partial T(x,t)}{\partial x}\right|_{x=0} = 0 \quad \text{and/or} \quad \left.\frac{\partial T(x,t)}{\partial x}\right|_{x=L} = 0.$$

- The second type of boundary condition is convection, in which the heat flux to/from the surface is proportional to the difference between the surface temperature and an ambient fluid temperature T_∞

$$-\lambda^{\text{eff}} \left.\frac{\partial T(x,t)}{\partial x}\right|_{x=0} = h\Big(T_\infty - T(0,t)\Big)$$

$$\lambda^{\text{eff}} \left.\frac{\partial T(x,t)}{\partial x}\right|_{x=L} = h\Big(T_\infty - T(L,t)\Big),$$

  where h [W m^{-2} K^{-1}] is the heat transfer (or convection) coefficient. The value of h is a property of the flow conditions of the fluid in contact to the surface, not a property of the surface itself.

- A third type of boundary condition is radiation, which can become significant when the surface temperatures are relatively high.
- Heat transfer to the surface via radiation can typically be expressed as

$$-\lambda^{\text{eff}} \left.\frac{\partial T(x,t)}{\partial x}\right|_{x=0} = \epsilon\sigma\left(T_\infty^4 - T^4(0,t)\right)$$

$$\lambda^{\text{eff}} \left.\frac{\partial T(x,t)}{\partial x}\right|_{x=L} = \epsilon\sigma\left(T_\infty^4 - T^4(L,t)\right),$$

  where ϵ [unitless] is the surface emissivity and $\sigma = 5.670373 \times 10^{-8}\,\text{W}\,\text{m}^{-2}\,\text{K}^4$ is the Stefan–Boltzmann constant.
- The problem with this boundary condition is that temperature appears in the fourth power, which makes the problem nonlinear in T and eliminates most hopes of finding an analytical solution.
- One way to deal with this is to linearize the radiation rate law via a first-order Taylor series expansion, giving

$$T_\infty^4 - T_s^4 \approx 4T_\infty^3(T_\infty - T_s).$$

- The quantity $4\epsilon\sigma T_\infty^3$ can now be viewed as a linearized radiation heat transfer coefficient, denoted h_{rad}.

Change in parameter values via Arrhenius relationship

- Most model parameter values are temperature dependent.
- This is usually modeled by the (empirical) Arrhenius relationship, which relates some property of the cell at present temperature T, $\Phi(T)$, to that property at a reference temperature T_{ref}, Φ_{ref} via an exponential function with "activation energy" E_0:

$$\Phi(T) = \Phi_{\text{ref}} \exp\left[\frac{E_0}{R}\left(\frac{1}{T_{\text{ref}}} - \frac{1}{T}\right)\right].$$

7.4: Reduced order modeling: Transfer functions

- To create a reduced-order thermal model, we must be able to:
  1. Approximate the four heat-gen. terms, resulting in total heat gen. q.
  2. Use q to model change in cell average temperature.
  3. In real time, blend models created at different temperature setpoints to approximate the true model behavior.
- These are described in the following sections.

Gradient transfer functions

- All heat-gen. terms are nonlinear, so transfer functions don't exist.
- Further, they are products of terms which themselves are functions of $i_{\text{app}}(t)$, so are essentially functions of $i_{\text{app}}^2(t)$: truncating a Taylor-series expansion will not give linearized models that are helpful.
- An approach that does work well is to individually compute the quantities that are ultimately multiplied together to predict heat gen.
  - We already know how to compute ROMs of $j(z,t)$ and $\eta(z,t)$.
  - We now need to compute $\nabla\phi_s(z,t)$, $\nabla \ln c_e(x,t)$, and $\nabla\phi_e(x,t)$.
- We can find these terms via a transfer-function approach.

Gradient of $\phi_s(z,t)$

- Recall from Chap. 6 that we defined $\tilde{\phi}_s(z,t) = \phi_s(z,t) - \phi_s(0,t)$. Then, the gradient with respect to the spatial coordinate z can be written as

$$\nabla_z \tilde{\phi}_s(z,t) = \nabla_z \phi_s(z,t) - \nabla_z \phi_s(0,t)$$

$$\nabla_z \phi_s(z,t) = \nabla_z \tilde{\phi}_s(z,t),$$

since $\phi_s(0,t)$ is not a function of a spatial dimension.

- Therefore, if we can find a transfer function for $\nabla_z \tilde{\phi}_s(z,t)$, we can compute the gradient we need for computing solid Joule heat gen.
- Recall also from Chap. 6

$$\frac{\widetilde{\Phi}_s^{\text{neg}}(z,s)}{I_{\text{app}}(s)} = -\frac{L^{\text{neg}}\kappa_{\text{eff}}^{\text{neg}}\left(\cosh(\nu^{\text{neg}}(s)) - \cosh((z-1)\nu^{\text{neg}}(s))\right)}{A\sigma_{\text{eff}}^{\text{neg}}(\kappa_{\text{eff}}^{\text{neg}} + \sigma_{\text{eff}}^{\text{neg}})\nu^{\text{neg}}(s)\sinh(\nu^{\text{neg}}(s))} - \frac{L^{\text{neg}}\sigma_{\text{eff}}^{\text{neg}}\left(1 - \cosh(z\nu^{\text{neg}}(s)) + z\nu^{\text{neg}}(s)\sinh(\nu^{\text{neg}}(s))\right)}{A\sigma_{\text{eff}}^{\text{neg}}(\kappa_{\text{eff}}^{\text{neg}} + \sigma_{\text{eff}}^{\text{neg}})\nu^{\text{neg}}(s)\sinh(\nu^{\text{neg}}(s))}.$$

- Taking the derivative of this function with respect to z gives

$$\frac{\nabla_z \widetilde{\Phi}_s^{\text{neg}}(z,s)}{I_{\text{app}}(s)} = \frac{L^{\text{neg}}\left(\sigma_{\text{eff}}^{\text{neg}}\left(\sinh(z\upsilon^{\text{neg}}(s)) - \sinh(\upsilon^{\text{neg}}(s))\right)\right)}{A\sigma_{\text{eff}}^{\text{neg}}(\kappa_{\text{eff}}^{\text{neg}} + \sigma_{\text{eff}}^{\text{neg}})\sinh(\nu^{\text{neg}}(s))} + \frac{L^{\text{neg}}\left(\kappa_{\text{eff}}^{\text{neg}}\sinh((z-1)\upsilon^{\text{neg}}(s))\right)}{A\sigma_{\text{eff}}^{\text{neg}}(\kappa_{\text{eff}}^{\text{neg}} + \sigma_{\text{eff}}^{\text{neg}})\sinh(\nu^{\text{neg}}(s))}.$$

- The gradient with respect to x can be found as

$$\left.\frac{\nabla_x \widetilde{\Phi}_s^{\text{neg}}(z,s)}{I_{\text{app}}(s)}\right|_{\frac{x}{L^{\text{neg}}}} = \left(\frac{\partial z}{\partial x}\right)\left(\frac{\nabla_z \widetilde{\Phi}_s^{\text{neg}}\left(\frac{x}{L^{\text{neg}}},s\right)}{I_{\text{app}}(s)}\right) = \frac{1}{L^{\text{neg}}}\left(\frac{\nabla_z \widetilde{\Phi}_s^{\text{neg}}\left(\frac{x}{L^{\text{neg}}},s\right)}{I_{\text{app}}(s)}\right)$$

$$= \left.\frac{\sigma_{\text{eff}}^{\text{neg}}\left(\sinh(z\upsilon^{\text{neg}}(s)) - \sinh(\upsilon^{\text{neg}}(s))\right)}{A\sigma_{\text{eff}}^{\text{neg}}(\kappa_{\text{eff}}^{\text{neg}} + \sigma_{\text{eff}}^{\text{neg}})\sinh(\nu^{\text{neg}}(s))}\right|_{\frac{x}{L^{\text{neg}}}} + \left.\frac{\kappa_{\text{eff}}^{\text{neg}}\sinh((z-1)\upsilon^{\text{neg}}(s))}{A\sigma_{\text{eff}}^{\text{neg}}(\kappa_{\text{eff}}^{\text{neg}} + \sigma_{\text{eff}}^{\text{neg}})\sinh(\nu^{\text{neg}}(s))}\right|_{\frac{x}{L^{\text{neg}}}}.$$

- In the positive electrode, $\widetilde{\Phi}_s(z,s)$ and its gradient with respect to x must both be multiplied by -1, so the net effect is nil.

- The same basic transfer function is used for both electrodes, with the substitution of constants appropriate for each electrode, and with $z = (L^{\text{tot}} - x)/L^{\text{pos}}$ substituted in the positive electrode.

Gradient of $\ln c_e(x,t)$

- We need to be able to compute $\nabla \ln c_e(x,t)$ to find q_e. Note that

$$\nabla \ln c_e(x,t) = \frac{\nabla c_e(x,t)}{c_e(x,t)},$$

and as we already compute $c_e(x,t)$ as an output of the ROM, we need only to learn how to compute $\nabla c_e(x,t)$.

- Recall that $c_e(x,t) = \tilde{c}_e(x,t) + c_{e,0}$, so $\nabla c_e(x,t) = \nabla \tilde{c}_e(x,t)$. We have already derived a transfer function for $\tilde{c}_e(x,t)$, which we wrote as

$$\frac{\widetilde{C}_e(x,s)}{I_{\text{app}}(s)} = \sum_{n=1}^{M} \frac{\widetilde{C}_{e,n}(s)}{I_{\text{app}}(s)} \Psi(x;\lambda_n).$$

- As only the eigenfunctions in this summation are a function of x, the gradient can be found as

$$\frac{\nabla \widetilde{C}_e(x,s)}{I_{\text{app}}(s)} = \sum_{n=1}^{M} \frac{\widetilde{C}_{e,n}(s)}{I_{\text{app}}(s)} \left(\nabla \Psi(x;\lambda_n)\right).$$

- All of the hard work computing $\widetilde{C}_{e,n}(s)$ is reused; only change is that we must multiply these terms by the *gradients* of the original eigenfunctions, not by the eigenfunctions themselves.

- Recall that the eigenfunctions were defined by

$$\Psi(x;\lambda) = \begin{cases} \Psi^{\text{neg}}(x;\lambda), & 0 \le x < L^{\text{neg}}; \\ \Psi^{\text{sep}}(x;\lambda), & L^{\text{neg}} \le x < L^{\text{neg}} + L^{\text{sep}}; \\ \Psi^{\text{pos}}(x;\lambda), & L^{\text{neg}} + L^{\text{sep}} \le x \le L^{\text{tot}}. \end{cases}$$

where

$$\Psi^{\text{neg}}(x;\,\lambda) = k_1 \cos\left(\sqrt{\lambda\varepsilon_e^{\text{neg}}/D_{e,\text{eff}}^{\text{neg}}}x\right)$$

$$\Psi^{\text{sep}}(x;\,\lambda) = k_3 \cos\left(\sqrt{\lambda\varepsilon_e^{\text{sep}}/D_{e,\text{eff}}^{\text{sep}}}x\right) + k_4 \sin\left(\sqrt{\lambda\varepsilon_e^{\text{sep}}/D_{e,\text{eff}}^{\text{sep}}}x\right)$$

$$\Psi^{\text{pos}}(x;\,\lambda) = k_5 \cos\left(\sqrt{\lambda\varepsilon_e^{\text{pos}}/D_{e,\text{eff}}^{\text{pos}}}x\right) + k_6 \sin\left(\sqrt{\lambda\varepsilon_e^{\text{pos}}/D_{e,\text{eff}}^{\text{pos}}}x\right).$$

- Then,

$$\nabla\Psi^{\text{neg}}(x;\,\lambda) = -k_1\sqrt{\frac{\lambda\varepsilon_e^{\text{neg}}}{D_{e,\text{eff}}^{\text{neg}}}}\sin\left(\sqrt{\frac{\lambda\varepsilon_e^{\text{neg}}}{D_{e,\text{eff}}^{\text{neg}}}}x\right)$$

$$\nabla\Psi^{\text{sep}}(x;\,\lambda) = k_4\sqrt{\frac{\lambda\varepsilon_e^{\text{sep}}}{D_{e,\text{eff}}^{\text{sep}}}}\cos\left(\sqrt{\frac{\lambda\varepsilon_e^{\text{sep}}}{D_{e,\text{eff}}^{\text{sep}}}}x\right) - k_3\sqrt{\frac{\lambda\varepsilon_e^{\text{sep}}}{D_{e,\text{eff}}^{\text{sep}}}}\sin\left(\sqrt{\frac{\lambda\varepsilon_e^{\text{sep}}}{D_{e,\text{eff}}^{\text{sep}}}}x\right)$$

$$\nabla\Psi^{\text{pos}}(x;\,\lambda) = k_6\sqrt{\frac{\lambda\varepsilon_e^{\text{pos}}}{D_{e,\text{eff}}^{\text{pos}}}}\cos\left(\sqrt{\frac{\lambda\varepsilon_e^{\text{pos}}}{D_{e,\text{eff}}^{\text{pos}}}}x\right) - k_5\sqrt{\frac{\lambda\varepsilon_e^{\text{pos}}}{D_{e,\text{eff}}^{\text{pos}}}}\sin\left(\sqrt{\frac{\lambda\varepsilon_e^{\text{pos}}}{D_{e,\text{eff}}^{\text{pos}}}}x\right).$$

Gradient of $\phi_e(x,t)$

- To compute the gradient of $\phi_e(x,t)$, recall that we have previously defined $\tilde{\phi}_e(x,t) = \phi_e(x,t) - \phi_e(0,t)$.
- Therefore, $\nabla\tilde{\phi}_e(x,t) = \nabla\phi_e(x,t) - \nabla\phi_e(0,t)$, or

$$\nabla\phi_e(x,t) = \nabla\tilde{\phi}_e(x,t).$$

- Recall also that we wrote $\tilde{\phi}_e(x,t)$ as having two parts

$$\tilde{\phi}_e(x,t) = \left[\tilde{\phi}_e(x,t)\right]_1 + \left[\tilde{\phi}_e(x,t)\right]_2.$$

- The first part, $\left[\tilde{\phi}_e(x,t)\right]_1$, can be determined via transfer functions; the second part, $\left[\tilde{\phi}_e(x,t)\right]_2$, can be determined via known $c_e(x,t)$.

- Gradient of the first part can also be found via transfer functions; gradient of the second part will furthermore require $c_e(x,t)$.
- Let's continue to look at the first part. In the negative electrode,

$$\frac{[\widetilde{\Phi}_e(x,s)]_1}{I_{\text{app}}(s)} = -\frac{L^{\text{neg}}\sigma_{\text{eff}}^{\text{neg}}\left(\cosh\left(\frac{x}{L^{\text{neg}}}\nu^{\text{neg}}(s)\right)-1\right)}{A\kappa_{\text{eff}}^{\text{neg}}(\kappa_{\text{eff}}^{\text{neg}}+\sigma_{\text{eff}}^{\text{neg}})\nu^{\text{neg}}(s)\sinh(\nu^{\text{neg}}(s))} - \frac{x}{A(\kappa_{\text{eff}}^{\text{neg}}+\sigma_{\text{eff}}^{\text{neg}})} - \frac{L^{\text{neg}}\kappa_{\text{eff}}^{\text{neg}}\left(\cosh\left(\frac{(L^{\text{neg}}-x)}{L^{\text{neg}}}\nu^{\text{neg}}(s)\right)-\cosh(\nu^{\text{neg}}(s))\right)}{A\kappa_{\text{eff}}^{\text{neg}}(\kappa_{\text{eff}}^{\text{neg}}+\sigma_{\text{eff}}^{\text{neg}})\nu^{\text{neg}}(s)\sinh(\nu^{\text{neg}}(s))}.$$

- The corresponding gradient, computed with the aid of Mathematica, is

$$\frac{\nabla[\widetilde{\Phi}_e(x,s)]_1}{I_{\text{app}}(s)} = \frac{\kappa_{\text{eff}}^{\text{neg}}\left(\sinh\left(\frac{(L^{\text{neg}}-x)\nu^{\text{neg}}(s)}{L^{\text{neg}}}\right)-\sinh(\nu^{\text{neg}}(s))\right)}{A\kappa_{\text{eff}}^{\text{neg}}(\kappa_{\text{eff}}^{\text{neg}}+\sigma_{\text{eff}}^{\text{neg}})\sinh(\nu^{\text{neg}}(s))} - \frac{\sigma_{\text{eff}}^{\text{neg}}\sinh\left(\frac{x\nu^{\text{neg}}(s)}{L^{\text{neg}}}\right)}{A\kappa_{\text{eff}}^{\text{neg}}(\kappa_{\text{eff}}^{\text{neg}}+\sigma_{\text{eff}}^{\text{neg}})\sinh(\nu^{\text{neg}}(s))}.$$

- In the separator, we had

$$\frac{[\widetilde{\Phi}_e(x,s)]_1}{I_{\text{app}}(s)} = -\frac{L^{\text{neg}}\left((\sigma_{\text{eff}}^{\text{neg}}-\kappa_{\text{eff}}^{\text{neg}})\tanh\left(\frac{\nu^{\text{neg}}(s)}{2}\right)\right)}{A\kappa_{\text{eff}}^{\text{neg}}(\kappa_{\text{eff}}^{\text{neg}}+\sigma_{\text{eff}}^{\text{neg}})\nu^{\text{neg}}(s)} - \frac{L_{\text{neg}}}{A(\kappa_{\text{eff}}^{\text{neg}}+\sigma_{\text{eff}}^{\text{neg}})} - \frac{x-L^{\text{neg}}}{A\kappa_{\text{eff}}^{\text{sep}}}.$$

- The corresponding gradient is

$$\frac{\nabla[\widetilde{\Phi}_e(x,s)]_1}{I_{\text{app}}(s)} = -\frac{1}{A\kappa_{\text{eff}}^{\text{sep}}}.$$

- In the positive electrode, we had

$$\frac{[\widetilde{\Phi}_e(x,s)]_1}{I_{\text{app}}(s)} = -\frac{L^{\text{neg}}\left((\sigma_{\text{eff}}^{\text{neg}}-\kappa_{\text{eff}}^{\text{neg}})\tanh\left(\frac{\nu^{\text{neg}}(s)}{2}\right)\right)}{A\kappa_{\text{eff}}^{\text{neg}}(\kappa_{\text{eff}}^{\text{neg}}+\sigma_{\text{eff}}^{\text{neg}})\nu^{\text{neg}}(s)} - \frac{L_{\text{neg}}}{A(\kappa_{\text{eff}}^{\text{neg}}+\sigma_{\text{eff}}^{\text{neg}})}$$

$$- \frac{L^{\text{sep}}}{A\kappa_{\text{eff}}^{\text{sep}}} - \frac{L^{\text{pos}}\left(1 - \cosh\left(\frac{(L^{\text{neg}}+L^{\text{sep}}-x)}{L^{\text{pos}}}\nu^{\text{pos}}(s)\right)\right)}{A(\kappa_{\text{eff}}^{\text{pos}} + \sigma_{\text{eff}}^{\text{pos}})\sinh(\nu^{\text{pos}}(s))\nu^{\text{pos}}(s)}$$
$$- \frac{L^{\text{pos}}\sigma_{\text{eff}}^{\text{pos}}\left(\cosh\left(\nu^{\text{pos}}(s)\right) - \cosh\left(\frac{(L^{\text{tot}}-x)}{L^{\text{pos}}}\nu^{\text{pos}}(s)\right)\right)}{A\kappa_{\text{eff}}^{\text{pos}}(\kappa_{\text{eff}}^{\text{pos}} + \sigma_{\text{eff}}^{\text{pos}})\sinh(\nu^{\text{pos}}(s))\nu^{\text{pos}}(s)}$$
$$- \frac{(x - L^{\text{neg}} - L^{\text{sep}})}{A(\kappa_{\text{eff}}^{\text{pos}} + \sigma_{\text{eff}}^{\text{pos}})}.$$

- The corresponding gradient is

$$\frac{\nabla[\widetilde{\Phi}_e(x,s)]_1}{I_{\text{app}}(s)} = \frac{\kappa_{\text{eff}}^{\text{pos}}\left(\sinh\left(\frac{\nu^{\text{pos}}(s)(L^{\text{pos}}-L^{\text{tot}}+x)}{L^{\text{pos}}}\right) - \sinh(\nu^{\text{pos}}(s))\right)}{A\kappa_{\text{eff}}^{\text{pos}}(\kappa_{\text{eff}}^{\text{pos}} + \sigma_{\text{eff}}^{\text{pos}})\sinh(\nu^{\text{pos}}(s))}$$
$$- \frac{\sigma_{\text{eff}}^{\text{pos}}\sinh\left(\frac{(L^{\text{tot}}-x)\nu^{\text{pos}}(s)}{L^{\text{pos}}}\right)}{A\kappa_{\text{eff}}^{\text{pos}}(\kappa_{\text{eff}}^{\text{pos}} + \sigma_{\text{eff}}^{\text{pos}})\sinh(\nu^{\text{pos}}(s))}.$$

- Now, we focus on the second term of $\tilde{\phi}_e(x,t)$.

$$\left[\tilde{\phi}_e(x,t)\right]_2 = \frac{2RT(1-t_+^0)}{F}\left[\ln c_e(x,t) - \ln c_e(0,t)\right]$$
$$\nabla\left[\tilde{\phi}_e(x,t)\right]_2 = \frac{2RT(1-t_+^0)}{F}\left[\frac{\nabla c_e(x,t)}{c_e(x,t)} - \frac{\nabla c_e(0,t)}{c_e(0,t)}\right]$$
$$= \frac{2RT(1-t_+^0)}{F}\frac{\nabla c_e(x,t)}{c_e(x,t)}.$$

- As we already compute $c_e(x,t)$ as an output of the ROM, and we have seen how to compute $\nabla c_e(x,t)$, we have all the terms necessary to compute $\nabla[\tilde{\phi}_e(x,t)]_2$, and therefore we can compute $\nabla\phi_e(x,t)$.

7.5: ROM heat-generation terms: $q_r(z,t)$ and $q_i(z,t)$

- We are now ready to investigate different reduced-order approximations to the heat-generation terms.
- Depending on the accuracy requirements of an application, different approaches may be taken, with different computational demands.
- So, to illustrate the tradeoffs, we will use several examples in this section to compare the results predicted by the different approaches.
- We use the same basic cell as was used in the examples in Chap. 6.
- The three examples that we consider are:

  1. A 1C discharge pulse, then a charge pulse, around 50 % SOC;
  2. A full 1C discharge starting at 100 % state of charge; and
  3. A charge-neutral UDDS profile, around 60 % state of charge

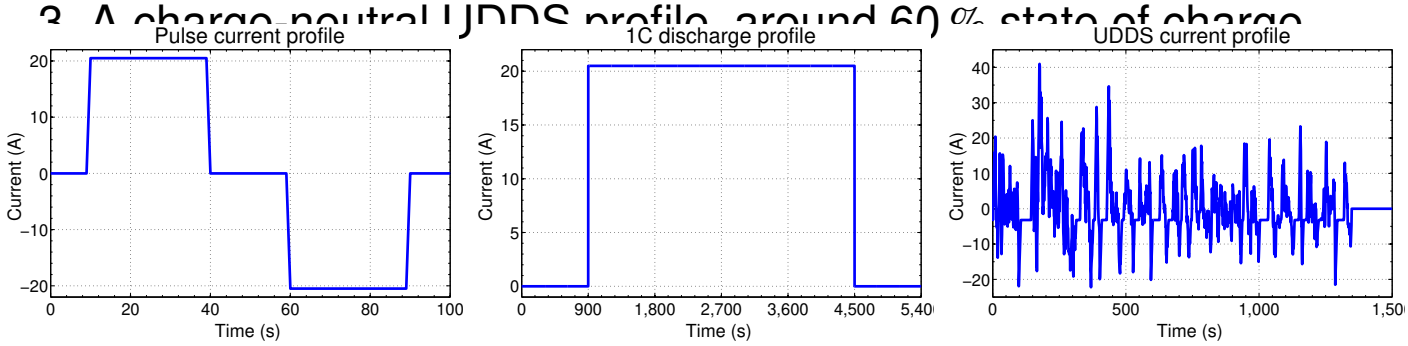

Reversible heat-generation term $q_r(z,t)$

- We first consider the reversible heat generation term, specialized to a single chemical reaction occurring at the solid–electrolyte boundary,

$$q_r(z,t) = a_s F T j(z,t) \frac{\partial U_{\text{ocp}}(c_{s,e}(z,t))}{\partial T},$$

  assuming that temperature is relatively constant across an electrode.

- We already have transfer functions for $j(z,t)$ and $c_{s,e}(z,t)$. We can approximate the average reversible heat gen. across the electrode as

$$\begin{aligned}\bar{q}_r(t) &= \frac{1}{L}\int_0^L a_s F T j(x/L,t)\frac{\partial U_{\text{ocp}}(c_{s,e}(x/L,t))}{\partial T}\,\mathrm{d}x \\ &= \int_0^1 a_s F T j(z,t)\frac{\partial U_{\text{ocp}}(c_{s,e}(z,t))}{\partial T}\,\mathrm{d}z \\ &\approx a_s F T \sum_i j(z_i,t)\frac{\partial U_{\text{ocp}}(c_{s,e}(z_i,t))}{\partial T}\Delta z_i.\end{aligned}$$

- That is, $j(z,t)$ and $c_{s,e}(z,t)$ are evaluated at a number of z locations across the electrode, the entropy function is evaluated at each $c_{s,e}$ point, and an approximation is made to the integral to compute the average heat generation using a rectangular integration summation.
- For an even better approximation, a trapezoidal integration can be performed, which uses different weighting constants for every z_i point.
- In the simulations that follow, we use five z_i points with trapezoidal integration in the results labeled "ROM1" through "ROM3."
- Computing $j(z,t)$ and $c_{s,e}(z,t)$ at multiple z locations incurs a fair amount of real-time computation in the $\boldsymbol{C}\boldsymbol{x}_k + \boldsymbol{D}\boldsymbol{i}_{\text{app}}$ step.
- It is possible to make a cruder approximation to $\bar{q}_r$ and reduce the amount of computation required.
- That is, if we assume $c_{s,e} \approx c_{\text{avg}}$ across the electrode, then we have

$$\begin{aligned}\bar{q}_r &= \int_0^1 a_s F T j(z,t)\frac{\partial U_{\text{ocp}}(c_{\text{avg}}(t))}{\partial T}\,\mathrm{d}z \\ &= a_s F T \frac{\partial U_{\text{ocp}}(c_{\text{avg}}(t))}{\partial T}\int_0^1 j(z,t)\,\mathrm{d}z\end{aligned}$$

$$= \frac{i_{\text{app}}(t)T}{A} \frac{\partial U_{\text{ocp}}(c_{\text{avg}}(t))}{\partial T}.$$

- In following simulations, we use this method in "ROM4" results.
- To compute $\bar{q}_r$, we must also know the partial-molar entropy.
  - For the negative electrode, we use the "graphite" curve from the earlier figure; for the positive electrode, we use the "LMO" curve.
- The figure shows sample results for the pulses test.
- Both ROM1 and ROM4 give similar predictions, primarily because the simulation was not long enough for significant gradients in the solid surface concentration to arise.

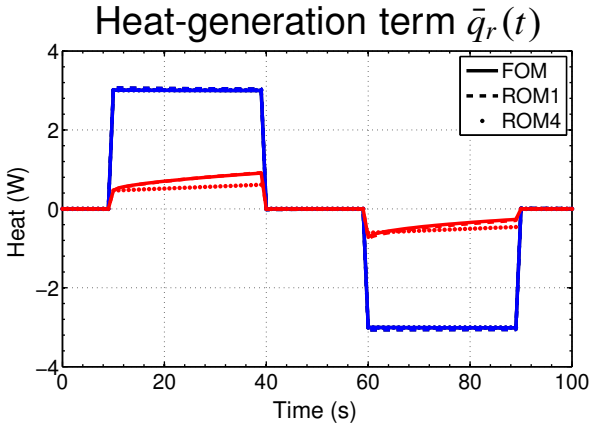

- Had they done so, ROM1 would be much better than ROM4.
- The choice of which ROM to use depends on the application.

Irreversible heat-generation term $q_i(z, t)$

- We next consider the irreversible heat generation term, specialized to a single chemical reaction occurring at the solid–electrolyte boundary,

$$q_i(z, t) = a_s F j(z, t) \eta(z, t).$$

- From Chap. 6, we have already found a transfer function for $j(z, t)$, and have seen how to compute $\eta(z, t)$ from a nonlinear relationship.
- We can approximate the average irreversible heat generation across the electrode as

$$\bar{q}_i(t) = \int_0^1 a_s F T j(z,t)\eta(z,t)\,\mathrm{d}z$$
$$\approx a_s F T \sum_i j(z_i,t)\eta(z_i,t)\Delta z_i.$$

- As before, we can also use a trapezoidal integration approximation.
- In the simulations that follow, we use five z_i points with trapezoidal integration in the results labeled "ROM1."
- For a reduction in computational complexity that incurs only a modest loss of accuracy, we can linearize the $\eta(z,t)$ term and recall $\eta(z,t) \approx F R_{\mathrm{ct}} j(z,t)$. This allows us to write

$$\bar{q}_i(t) \approx a_s F T R_{\mathrm{ct}} \sum_i j^2(z_i,t)\Delta z_i.$$

- The advantage of this form is that it is the product of two two terms found via fully linear transfer functions.
- We will see this form in the other heat-generation terms as well, so we take some time to examine it in general.
- Consider a generic heat-generation term, in discrete time

$$q[z,k] = y_1[z,k]\, y_2[z,k],$$

where $y_1[z,k]$ and $y_2[z,k]$ are both purely linear terms computed as output from the state-space reduced-order model (that is, there are no nonlinear corrections applied to the terms). Then,

$$\bar{q}[z,k] = \int_0^1 y_1[z,k]\, y_2[z,k]\,\mathrm{d}z$$
$$= \int_0^1 [\boldsymbol{C}_1\boldsymbol{x}[k] + \boldsymbol{D}_1 u[k]]\,[\boldsymbol{C}_2\boldsymbol{x}[k] + \boldsymbol{D}_2 u[k]]\,\mathrm{d}z.$$

- The terms written inside square brackets are scalars, so are equal to their own transpose.
- This allows us to write

$$\begin{aligned}\bar{q}[z,k] &= \int_0^1 \left[\boldsymbol{x}^T[k]\boldsymbol{C}_1^T + u^T[k]\boldsymbol{D}_1^T\right]\left[\boldsymbol{C}_2\boldsymbol{x}[k] + \boldsymbol{D}_2 u[k]\right]\,\mathrm{d}z \\ &= \boldsymbol{x}^T[k]\underbrace{\left\{\int_0^1 \boldsymbol{C}_1^T\boldsymbol{C}_2\,\mathrm{d}z\right\}}_{\{\boldsymbol{CC}\}}\boldsymbol{x}[k] + u^T[k]\underbrace{\left\{\int_0^1 \boldsymbol{D}_1^T\boldsymbol{D}_2\,\mathrm{d}z\right\}}_{\{\boldsymbol{DD}\}}u[k] \\ &\quad + \boldsymbol{x}^T[k]\underbrace{\left\{\int_0^1 \boldsymbol{C}_1^T\boldsymbol{D}_2 + \boldsymbol{C}_2^T\boldsymbol{D}_1\,\mathrm{d}z\right\}}_{\{\boldsymbol{CD}\}}u[k] \\ &= \boldsymbol{x}^T[k]\{\boldsymbol{CC}\}\boldsymbol{x}[k] + \boldsymbol{x}^T[k]\{\boldsymbol{CD}\}u[k] + u^T[k]\{\boldsymbol{DD}\}u[k].\end{aligned}$$

- The $\boldsymbol{C}$ and $\boldsymbol{D}$ matrices are produced by the DRA from the appropriate transfer functions, and the integrals are approximated from these matrices using a one-time computation, resulting in constant pre-computed $\{\boldsymbol{CC}\}$, $\{\boldsymbol{CD}\}$, and $\{\boldsymbol{DD}\}$ matrices.
- Expressing the heat generation in this form allows us to consider a number of different approximations to the original result, at different levels of complexity.
  - The integral involving $\boldsymbol{C}_1^T\boldsymbol{C}_2$ requires the most computations, resulting in an $n \times n$ output at every z value.
  - The integral involving $\boldsymbol{C}_i^T\boldsymbol{D}_j$ has fewer computations, resulting in an $n \times 1$ vector for every z value.
  - The integral involving $\boldsymbol{D}_1^T\boldsymbol{D}_2$ has the fewest computations, resulting in a 1×1 scalar at every z value.

- If we are able to drop terms from the approximation without losing too much fidelity, we can reduce the real-time computation load of estimating a heat-generation term.
- In the following, "ROM2" simulations use the full expression

$$\bar{q}_i[z,k] = \boldsymbol{x}^T[k]\,\{\boldsymbol{CC}\}\,\boldsymbol{x}[k] + \boldsymbol{x}^T[k]\,\{\boldsymbol{CD}\}\,i_{\text{app}}[k] + \{\boldsymbol{DD}\}\,i^2_{\text{app}}[k].$$

- "ROM3" and "ROM4" simulations use a simpler computation

$$\bar{q}_i[z,k] = \{\boldsymbol{DD}\}\,i^2_{\text{app}}[k].$$

- Note that this corresponds to an "$i^2 \times R$" type of heat generation we would expect from a lumped resistance.
- The other scenarios give better approximations to the heat generation within an electrode, which is a distributed system.
- In the ROM2 through ROM4 results that follow for the irreversible heat-generation term, we selected $y_1[z,k] = y_2[z,k] = j[z,k]$ and computed

$$\bar{q}_i(t) \approx a_s F T R_{\text{ct}} \int_0^1 y_1[z,k]\,y_2[z,k]\,\mathrm{d}z,$$

  using the three different above.
- The figure shows sample results for the pulses test.
- In this case, ROM1 is significantly better than ROM2, which itself is significantly better than ROM3.
- The fidelity of predictions required by the application will dictate which ROM to use.

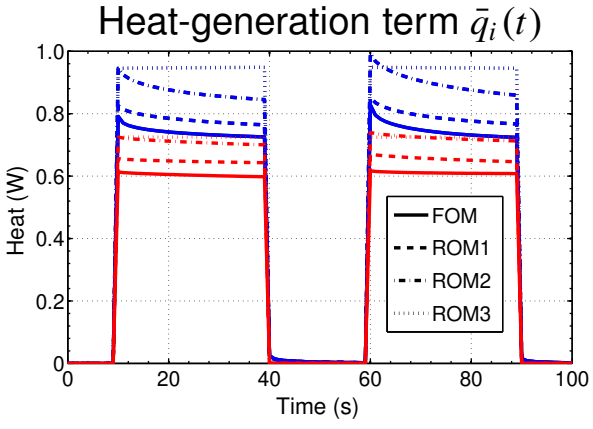

7.6: ROM heat-generation terms: $q_s(z,t)$ and $q_e(z,t)$

Joule heating in solid term $q_s(z,t)$

- We now consider the heat-generation term corresponding to Joule heating in the solid, expressed as $q_s = \sigma_{\text{eff}}(\nabla\phi_s \cdot \nabla\phi_s)$.
- We have already seen that we can express $\nabla\phi_s$ as a purely linear transfer function, so we can use the same approaches as we did with irreversible heat generation.
- In the simulations that follow, we select $y_1[z,k] = y_2[z,k] = \nabla\phi_s[z,k]$ and compute

$$\bar{q}_s(t) = \sigma_{\text{eff}} \int_0^1 y_1[z,k]\, y_2[z,k]\, \mathrm{d}z.$$

- Results labeled “ROM1” or “ROM2” use the full expression

$$\bar{q}_s[z,k] = \boldsymbol{x}^T[k]\,\{\boldsymbol{CC}\}\,\boldsymbol{x}[k] + \boldsymbol{x}^T[k]\,\{\boldsymbol{CD}\}\,i_{\text{app}}[k] + \{\boldsymbol{DD}\}\,i^2_{\text{app}}[k].$$

- Results labeled “ROM3” and “ROM4” use a simpler computation

$$\bar{q}_s[z,k] = \{\boldsymbol{DD}\}\,i^2_{\text{app}}[k].$$

- The figure shows sample results for the pulses test.
- The solid line shows the full-order model result, and the decorated lines show different reduced-order model results.

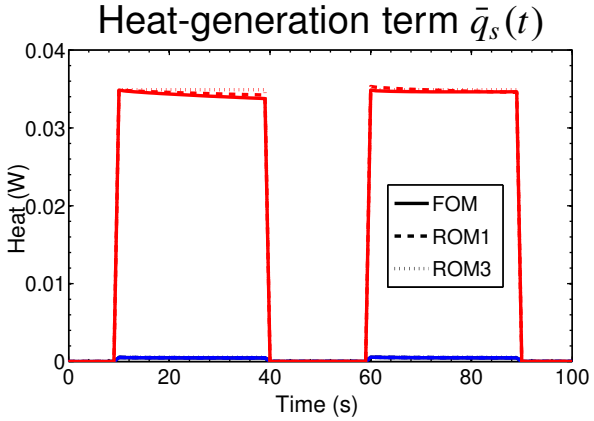

- In this case, all ROMS produce nearly indistinguishable results.
- Furthermore, a close examination of the vertical scale shows that the $\bar{q}_s(t)$ term is by far the smallest heat-generation term, so even large

relative errors are not significant when total heat generation is computed.

- Therefore, ROM3 is probably sufficient for most applications.

Joule heating in electrolyte term $q_e(x,t)$

- Finally, we consider the heat-generation term corresponding to Joule heating in the electrolyte.
- We take a few steps to convert it into a combination of signals at our disposal:

$$
\begin{aligned}
q_e &= \kappa_{\text{eff}}(\nabla\phi_e \cdot \nabla\phi_e) + \kappa_{D,\text{eff}}(\nabla \ln c_e \cdot \nabla\phi_e) \\
&= \kappa_{\text{eff}} \left(\left(\nabla[\tilde{\phi}_e]_1 \right)^2 + 2 \left(\nabla[\tilde{\phi}_e]_1 \nabla[\tilde{\phi}_e]_2 \right) + \left(\nabla[\tilde{\phi}_e]_2 \right)^2 \right) \\
&\quad + \kappa_{D,\text{eff}} \left(\frac{\nabla \tilde{c}_e}{c_e} \left(\nabla[\tilde{\phi}_e]_1 + \nabla[\tilde{\phi}_e]_2 \right) \right) \\
&= \kappa_{\text{eff}} \left(\left(\nabla[\tilde{\phi}_e]_1 \right)^2 + \frac{4RT(1-t_+^0)}{Fc_e} \left(\nabla[\tilde{\phi}_e]_1 \nabla \tilde{c}_e \right) + \left(\frac{2RT(1-t_+^0)\nabla \tilde{c}_e}{Fc_e} \right)^2 \right) \\
&\quad + \kappa_{\text{eff}} \left(\frac{2RT(t_+^0-1)}{F} \frac{\nabla \tilde{c}_e}{c_e} \left(\nabla[\tilde{\phi}_e]_1 + \frac{2RT(1-t_+^0)\nabla \tilde{c}_e}{Fc_e} \right) \right) \\
&= \kappa_{\text{eff}} \left(\nabla[\tilde{\phi}_e]_1 \right)^2 - \frac{\kappa_{D,\text{eff}}}{c_e} \nabla[\tilde{\phi}_e]_1 \nabla \tilde{c}_e .
\end{aligned}
$$

- To compute this result, we will need to have the DRA produce a ROM that can generate $\nabla[\tilde{\phi}_e]_1$, $\tilde{c}_e$, and $\nabla \tilde{c}_e$ at different locations across the cell, in order to create proper averages.
- For best results, we use $\kappa_{\text{eff}}(c_e(x,t))$ instead of the $\kappa_{\text{eff}}(c_{e,0})$ that we usually use.

- Furthermore, we recognize that the denominator of the transfer function for $\nabla[\tilde{\phi}_e]_1$ in all regions of the cell includes a κ_{eff} term.
- The DRA-produced ROM uses $\kappa_{\text{eff}}(c_{e,0})$ when making the linearized transfer function.
- However for best results, the output of the ROM should be multiplied by $\kappa_{\text{eff}}(c_{e,0})/\kappa_{\text{eff}}(c_e(x,t))$ since κ_{eff} is a strong function of c_e and $\nabla[\tilde{\phi}_e]_1$ is a strong function of κ_{eff}.
- Writing this out more explicitly, the heat-generation terms used for "ROM1" results presented below use

$$q_e(x,t) = \kappa_{\text{eff}}(c_e(x,t)) \left(\frac{\kappa_{\text{eff}}\,(c_{e,0})}{\kappa_{\text{eff}}(c_e(x,t))} \nabla[\tilde{\phi}_e]_1 \right)^2 - \frac{\kappa_{D,\text{eff}}}{c_e(x,t)} \nabla[\tilde{\phi}_e]_1 \nabla \tilde{c}_e.$$

- A simpler version assumes that $c_e(x,t) \approx c_{e,0}$. Results for "ROM2" through "ROM4" assume linearized results

$$q_e(x,t) = \kappa_{\text{eff}} \left(\nabla[\tilde{\phi}_e]_1 \right)^2 - \frac{\kappa_{D,\text{eff}}}{c_{e,0}} \nabla[\tilde{\phi}_e]_1 \nabla \tilde{c}_e.$$

- Then, the method from Section 7.5 can be used on both parts of this expression.
  - Results for "ROM2" use the full linearized expression;
  - Results for "ROM3" and "ROM4" retains only the $\{\boldsymbol{DD}\}$ terms.
- The figure shows sample results for the pulses test.
- The solid line shows the full-order model result, and the decorated lines show different reduced-order model results.

Heat-generation term $\bar{q}_e(t)$

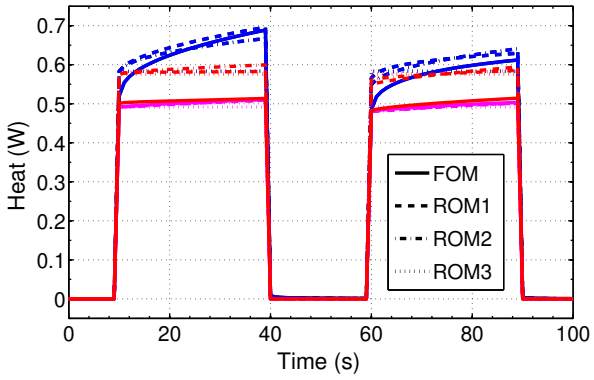

- In this case, all ROMs gave fairly similar predictions to each other, although ROM1 appears to be more robust over a variety of simulation scenarios.
- As a point of comparison, the total heat generated is modeled and displayed for the pulses and 1C discharge scenarios.

Total heat gen., $\bar{q}_i(t) + \bar{q}_r(t) + \bar{q}_s(t) + \bar{q}_e(t)$

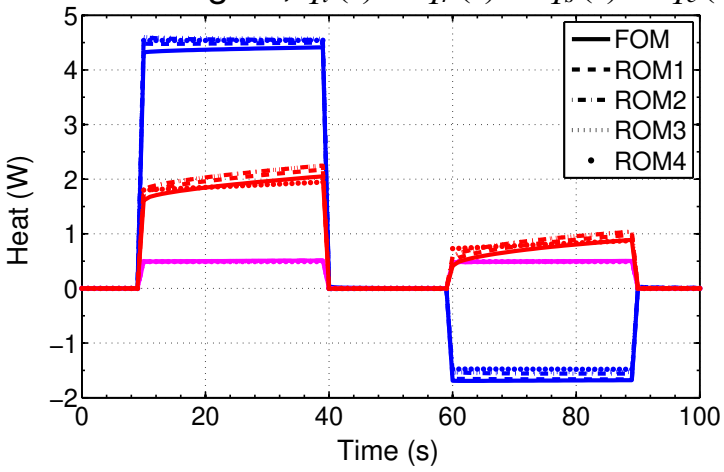

Total heat gen., $\bar{q}_i(t) + \bar{q}_r(t) + \bar{q}_s(t) + \bar{q}_e(t)$

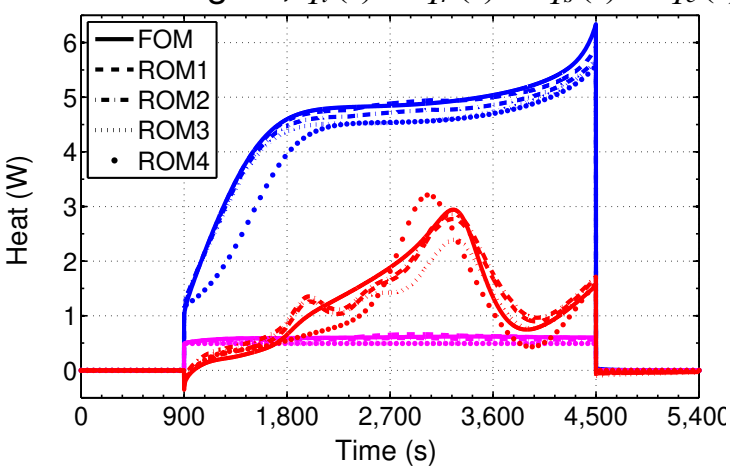

- We see that the predictions of the ROMs are quite similar. The only large discrepancy is with ROM4 for the 1C discharge case, and this error is due to the crude model of $\bar{q}_r(t)$.

7.7: Heat flux terms

- Now that we have seen how to approximate the heat-generation terms of the thermal model, we turn our attention to modeling heat flux, leading to an expression for average cell temperature.
- We start with underlying PDE

$$\rho c_P \frac{\partial T(x,t)}{\partial t} = \nabla \cdot (\lambda \nabla T(x,t)) + q(x,t),$$

with convective boundary condition

$$-\lambda \left. \frac{\partial T(x,t)}{\partial x} \right|_{x=0} = h(T_\infty - T(0,t)).$$

$$\lambda \left. \frac{\partial T(x,t)}{\partial x} \right|_{x=L} = h\Big(T_\infty - T(L,t)\Big),$$

- The constants ρ, c_P, and λ may be different in the three regions of the cell, but are assumed to be homogeneous within each region.
- Also, a radiative boundary condition may be approximated using

$$T_\infty^4 - T_s^4 \approx 4T_\infty^3 (T_\infty - T_s),$$

as discussed earlier.

- To solve this PDE, we might consider using separation of variables, as we did when exploring the PDE governing the concentration of lithium in the electrolyte, $c_e(x,t)$ in Chap. 6.
- However, since temperature tends to be fairly uniform across the x dimension of the cell, we use a simpler approach here, which is sufficient if all we want is average temperature of the cell and not an accurate model of the entire profile of $T(x,t)$.

- Assume that we can closely approximate $T(x,t)$ as

$$T(x,t) \approx T_\infty + a(t) + b(t)\sin\left(\frac{\pi x}{L^{\text{tot}}}\right).$$

- Then, the derivatives that we need to solve the PDE can be written as

$$\frac{\partial T(x,t)}{\partial t} = \frac{\mathrm{d}a(t)}{\mathrm{d}t} + \frac{\mathrm{d}b(t)}{\mathrm{d}t}\sin\left(\frac{\pi x}{L^{\text{tot}}}\right)$$
$$\frac{\partial T(x,t)}{\partial x} = \frac{\pi}{L^{\text{tot}}}b(t)\cos\left(\frac{\pi x}{L^{\text{tot}}}\right)$$
$$\frac{\partial^2 T(x,t)}{\partial x^2} = -\left(\frac{\pi}{L^{\text{tot}}}\right)^2 b(t)\sin\left(\frac{\pi x}{L^{\text{tot}}}\right).$$

- Inserting the assumed form of solution into the boundary condition at $x = 0$ gives

$$-\lambda\,\frac{\pi}{L^{\text{tot}}}b(t)\cos\left(\frac{\pi x}{L^{\text{tot}}}\right)\Big|_{x=0} = h(T_\infty - (T_\infty + a(t)))$$
$$-\lambda\frac{\pi}{L^{\text{tot}}}b(t) = -ha(t)$$
$$b(t) = \frac{hL^{\text{tot}}}{\lambda\pi}a(t).$$

- Evaluating the PDE with the assumed form of solution gives

$$\rho c_P\left[\frac{\mathrm{d}a(t)}{\mathrm{d}t} + \frac{hL^{\text{tot}}}{\lambda\pi}\frac{\mathrm{d}a(t)}{\mathrm{d}t}\sin\left(\frac{\pi x}{L^{\text{tot}}}\right)\right] = -\lambda\left(\frac{\pi}{L^{\text{tot}}}\right)^2\left(\frac{hL^{\text{tot}}}{\lambda\pi}\right)a(t)\sin\left(\frac{\pi x}{L^{\text{tot}}}\right) + q(x,t)$$
$$\rho c_P\left[1 + \frac{hL^{\text{tot}}}{\lambda\pi}\sin\left(\frac{\pi x}{L^{\text{tot}}}\right)\right]\frac{\mathrm{d}a(t)}{\mathrm{d}t} = -\left(\frac{\pi h}{L^{\text{tot}}}\right)a(t)\sin\left(\frac{\pi x}{L^{\text{tot}}}\right) + q(x,t).$$

- We will use this functional form as a basis for finding average cell temperature.

- To do so, we average both sides of the equation

$$\frac{1}{L^{\text{tot}}}\int_0^{L^{\text{tot}}} \rho c_P\left[1+\frac{hL^{\text{tot}}}{\lambda\pi}\sin\left(\frac{\pi x}{L^{\text{tot}}}\right)\right]\mathrm{d}x\,\frac{\mathrm{d}a(t)}{\mathrm{d}t} = -\left(\frac{\pi h}{L^{\text{tot}}}\frac{2}{\pi}\right)a(t)+\bar{q}(t),$$

where

$$\bar{q}(t) = \frac{1}{L^{\text{tot}}}\int_0^{L^{\text{tot}}} q(x,t)\,\mathrm{d}x,$$

and we have used

$$\frac{1}{L^{\text{tot}}}\int_0^{L^{\text{tot}}} \sin\left(\frac{\pi x}{L^{\text{tot}}}\right)\,\mathrm{d}x = \frac{2}{\pi}.$$

- We re-write this as

$$\frac{\mathrm{d}a(t)}{\mathrm{d}t} = -\left(\frac{2h}{k_q L^{\text{tot}}}\right)a(t)+\frac{1}{k_q}\bar{q}(t),$$

where the constant

$$\begin{aligned}
k_q &= \frac{1}{L^{\text{tot}}}\int_0^{L^{\text{tot}}} \rho c_P\left[1+\frac{hL^{\text{tot}}}{\lambda\pi}\sin\left(\frac{\pi x}{L^{\text{tot}}}\right)\right]\mathrm{d}x \\
&= \frac{1}{L^{\text{tot}}}\Bigg[\rho^{\text{neg}}c_P^{\text{neg}}\left(\frac{h(L^{\text{tot}})^2}{\lambda^{\text{neg}}\pi^2}\left(1-\cos\left(\frac{\pi L^{\text{neg}}}{L^{\text{tot}}}\right)\right)\right) \\
&\quad + \rho^{\text{sep}}c_P^{\text{sep}}\left(\frac{h(L^{\text{tot}})^2}{\lambda^{\text{sep}}\pi^2}\left(\cos\left(\frac{\pi L^{\text{neg}}}{L^{\text{tot}}}\right)-\cos\left(\frac{\pi(L^{\text{neg}}+L^{\text{sep}})}{L^{\text{tot}}}\right)\right)\right) \\
&\quad + \rho^{\text{pos}}c_P^{\text{pos}}\left(\frac{h(L^{\text{tot}})^2}{\lambda^{\text{pos}}\pi^2}\left(1+\cos\left(\frac{\pi(L^{\text{neg}}+L^{\text{sep}})}{L^{\text{tot}}}\right)\right)\right) \\
&\quad + \rho^{\text{neg}}c_P^{\text{neg}}L^{\text{neg}}+\rho^{\text{sep}}c_P^{\text{sep}}L^{\text{sep}}+\rho^{\text{pos}}c_P^{\text{pos}}L^{\text{pos}}\Bigg].
\end{aligned}$$

- Recalling that

$$\begin{aligned}
T(x,t) &\approx T_\infty + a(t) + b(t)\sin\left(\frac{\pi x}{L^{\text{tot}}}\right) \\
&= T_\infty + a(t)\left[1+\frac{hL^{\text{tot}}}{\lambda\pi}\sin\left(\frac{\pi x}{L^{\text{tot}}}\right)\right],
\end{aligned}$$

we can compute an average temperature

$$T_{\text{avg}}(t) = T_\infty + \frac{a(t)}{L^{\text{tot}}} \int_0^{L^{\text{tot}}} 1 + \frac{hL^{\text{tot}}}{\lambda\pi} \sin\left(\frac{\pi x}{L^{\text{tot}}}\right) \, \mathrm{d}x$$

$$= T_\infty + C_q a(t),$$

where the constant

$$C_q = \frac{1}{L^{\text{tot}}} \int_0^{L^{\text{tot}}} 1 + \frac{hL^{\text{tot}}}{\lambda\pi} \sin\left(\frac{\pi x}{L^{\text{tot}}}\right) \, \mathrm{d}x$$

$$= \frac{1}{L^{\text{tot}}}\Bigg[\left(L^{\text{neg}} + \frac{h(L^{\text{tot}})^2}{\lambda^{\text{neg}}\pi^2}\left(1 - \cos\left(\frac{\pi L^{\text{neg}}}{L^{\text{tot}}}\right)\right)\right)$$

$$+ \left(L^{\text{sep}} + \frac{h(L^{\text{tot}})^2}{\lambda^{\text{sep}}\pi^2}\left(\cos\left(\frac{\pi L^{\text{neg}}}{L^{\text{tot}}}\right) - \cos\left(\frac{\pi (L^{\text{neg}} + L^{\text{sep}})}{L^{\text{tot}}}\right)\right)\right)$$

$$+ \left(L^{\text{pos}} + \frac{h(L^{\text{tot}})^2}{\lambda^{\text{pos}}\pi^2}\left(1 + \cos\left(\frac{\pi (L^{\text{neg}} + L^{\text{sep}})}{L^{\text{tot}}}\right)\right)\right)\Bigg]$$

$$= 1 + \frac{hL^{\text{tot}}}{\pi^2}\Bigg[\frac{1}{\lambda^{\text{neg}}}\left(1 - \cos\left(\frac{\pi L^{\text{neg}}}{L^{\text{tot}}}\right)\right)$$

$$+ \frac{1}{\lambda^{\text{sep}}}\left(\cos\left(\frac{\pi L^{\text{neg}}}{L^{\text{tot}}}\right) - \cos\left(\frac{\pi (L^{\text{neg}} + L^{\text{sep}})}{L^{\text{tot}}}\right)\right)$$

$$+ \frac{1}{\lambda^{\text{pos}}}\left(1 + \cos\left(\frac{\pi (L^{\text{neg}} + L^{\text{sep}})}{L^{\text{tot}}}\right)\right)\Bigg].$$

- Converting to discrete time, we have the one-state ODE model for cell average temperature

$$a[k+1] = A_q a[k] + B_q \bar{q}[k]$$

$$T_{\text{avg}}[k] = C_q a[k] + T_\infty,$$

where

$$A_q = \exp\left(-\frac{2h}{k_q L^{\text{tot}}}\Delta t\right)$$

$$B_q = \begin{cases} -\dfrac{L^{\text{tot}}}{2h}\left(A_q - 1\right), & h \neq 0 \\ \dfrac{\Delta t}{k_q} & h = 0. \end{cases}$$

- Results of simulations to test the heat-flux ROM are shown below.
- In each figure, three different simulation scenarios are shown:
  - One for convection coefficient $h = 0$ (modeling the perfectly insulated or adiabatic case, with no heat transfer to or from the environment);
  - One with $h = 5$ (modeling natural convection); and
  - One with $h = 25$ (modeling forced air convection).
- In the first figure, we see the results for the pulse test.

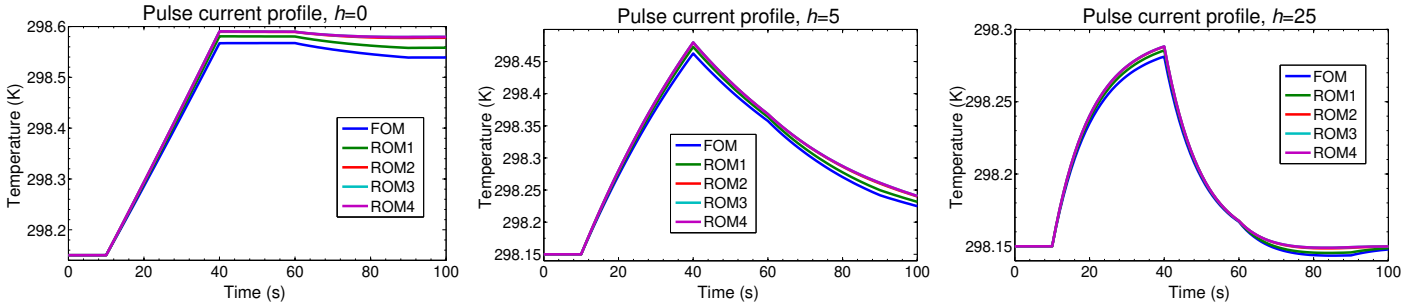

- All ROMs agree with the FOM results to within less than one degree over the entire simulation.
  - ROM1 is somewhat better than the others, but they are all similar.
- In the next figure, we see the results for the 1C discharge test.

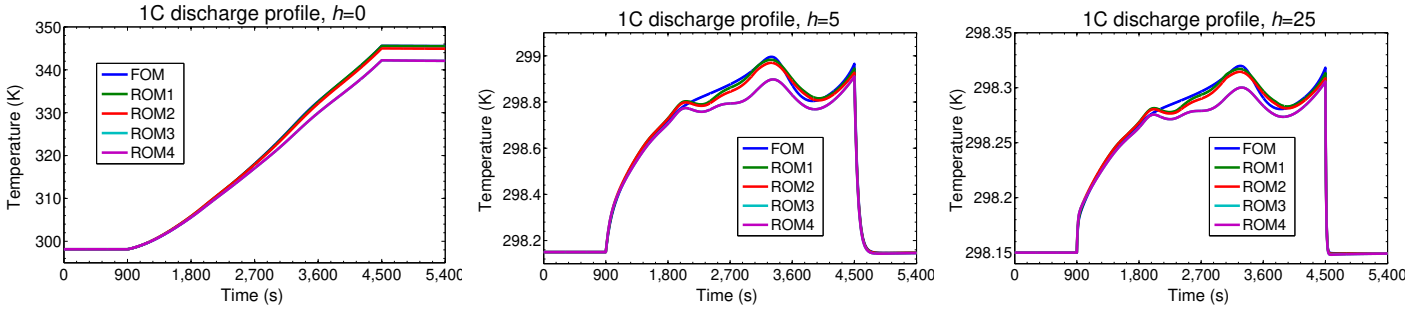

- Here, all ROMs do quite well again, although ROM4 is noticeably worse than the others.
  - This is due to the crude approximation of $\bar{q}_r(t)$.

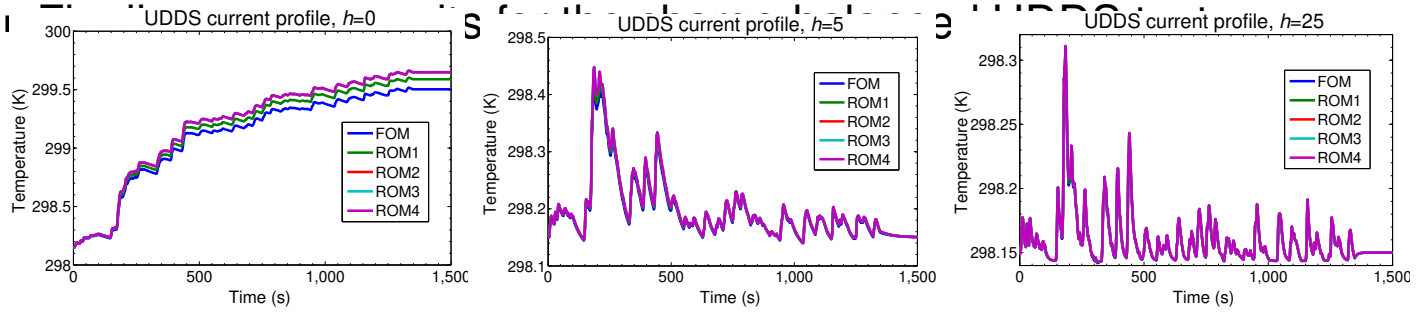

- Again, all ROMs do quite well. ROM1 slightly outperforms the others, but perhaps not enough to justify the additional complexity.

Wide operating range

- A coupled electrochemical-thermal lithium-ion battery-cell model can be created by combining the techniques we have seen to date.
- First, the Arrhenius equation is used to find parameter values at different temperature setpoints, and the DRA is used off-line to produce ROMs at different state-of-charge and temperature setpoints.
- Then, while the cell model is operating, the electrochemical model updates state of charge, and the thermal model updates temperature.
- $\widehat{\boldsymbol{A}}_k$, $\widehat{\boldsymbol{B}}_k$, $\widehat{\boldsymbol{C}}_k$, and $\widehat{\boldsymbol{D}}_k$ matrices used in real time are continuously updated via model-blending approach.

Where from here

- We now have methods for constructing and simulating reduced-order coupled electrochemical-thermal models of lithium-ion cells.

- We have found that these methods work quite well.
- One remaining challenge is the requirement of a method to identify all the physics-based parameters of the models.
  - At the moment, cell tear-down and specialized experiments to measure individual parameters are necessary.
  - Methods are being developed that avoid this requirement.
- The models are now ready for application. In *ECE5720: Battery Management and Control*, we discuss practical applications of battery models to the problems of proper battery management and control.
  - We consider the functions of a battery management system,
  - We briefly review battery cell models and extend them to be able to simulate of battery packs,
  - We look at cell state estimation and battery health estimation,
  - We discuss cell balancing requirements and methods,
  - We examine voltage-based power limit estimation,
  - We then expand our physics-based cell models to include descriptions of aging mechanisms and degradation models and look at optimized controls for power estimation that maximize battery output while minimizing the incremental aging.